International Society for Rock Mechanics and Rock Engineering
Norwegian Group for Rock Mechanics

ISRM International Symposium
Eurock 2025 – Expanding the Underground Space
Trondheim, Norway, 16-20 June
ISBN 978-82-8208-079-8

Experimental and Numerical Analysis of Discrete Joint around Circular Hole

R. Kumar, M. Mishra, T. Bhandari, S. Sarkar
Indian Institute of Technology Kharagpur, Kharagpur, India
rkumar@mining.iitkgp.ac.in

Abstract

Rock mass behavior in tunneling and mining has been paramount in geotechnical engineering, driving extensive research and advancements in experimental techniques and simulation tools. In this study, the effect of a single joint around a circular hole is studied numerically and in the laboratory. For this purpose, two sandstone samples of 10 cm x 10 cm x 5 cm are taken, and a circular hole of 2.1 cm is created at the center of the sample. Artificial discontinuity is inscribed in the specimen at 30° and 45° angles. Cut pieces of the sandstone samples are attached with a mixture of Portland cement and water. These prepared samples are uniaxially loaded in compression, and an LVDT is used to measure horizontal displacement caused by the joint. Shear stiffness, normal stiffness, and dilation of the joint are determined using laboratory data by transforming the obtained horizontal and vertical displacement along the joint.

Numerical simulation is performed using finite element method (FEM) based RS-3 software. The Mohr-coulomb failure criterion for rock and joint is used in the simulation. The values of shear stiffness and normal stiffness are used as input properties for the joint. The cohesion and internal angle of friction of the joint are determined by an iterative approach until the horizontal displacement of the sample is in accordance with laboratory results with minimal error. The cohesion is found at 200 kPa for the 30° joint and 75 kPa for the 45° joint. The internal angle of friction of the joint is found to be 35° for both cases. This study aims to quantify the cohesion, internal friction angle, shear stiffness, and normal stiffness of joints through a combination of experimental and numerical approaches.

Keywords

Circular hole, Discrete joint, Shear stiffness, Finite Element Method

ISRM

NBG

1 Introduction

In rock mass, discontinuities play a vital role in causing instability in the tunnels, dam foundations, mines, slopes, etc. Estimating rock mass properties is critical for designing and constructing geotechnical structures in rock mass (Kumar and Verma 2016). The anisotropic nature of rock mass makes it difficult to understand its mechanical behavior under various loading conditions. Joint, being the most prominent discontinuity as it influences the rock mass mechanical characteristics and engineering behaviors, governing the overall stability of geotechnical structures (Zhang et al. 2023). The most important joint properties are normal stiffness (K_{nn}) and shear stiffness (K_{ss}), which are determined in the laboratory and used as input parameters for the numerical modeling of the rock mass (Fan et al. 2024).

In practical scenarios, discontinuities are often accompanied by geotechnical developments such as openings and excavations, making their behavior more complex to simulate. The analytical solutions for normal and shear stress along the joint plane in the vicinity of a circular opening are derived using stress transformation equations (Brady and Brown 2006; Deb and Verma 2016). Aswad et al. (2020) investigated the influence of different joint orientations on rock failure mechanisms. Their study reveals that joint orientation can significantly affect the stress distribution within rock masses. The laboratory method for determining joint stiffness generally involves a direct shear test under a constant normal load or via a uniaxial compression test (Dang et al. 2017). Conventionally, linear variable differential transducers (LVDTs) (Brown and Scholz 1986) and strain gauges (Daemen et al. 2004) are used to measure the axial and lateral deformation along the joint, and the stress displacement trend is used to estimate the stiffness of the joint.

Pertaining to the complexity involved in the modeling of rock masses, various researchers have attempted to simulate the rock joint behavior using a numerical modeling approach. As discontinuities cannot be simulated with conventional continuum modeling techniques, researchers have developed advanced numerical procedures to deal with such situations. Over the past few decades, the discontinuities have been handled using techniques such as the Extended Finite Element Method (Deb and Das 2010), Bonded Particle Model (Park and Song 2009; Dong et al. 2022) to name a few.

This study aims to showcase the applicability of numerical modeling to estimate the joint properties such as cohesion and internal angle of friction using the experimental data for complex structures such as discontinuities around circular openings. The paper is structured as follows: Section 2 demonstrates the laboratory experiment conducted on jointed and holed rock samples, followed by its numerical modeling in Section 3. Finally, Section 4 shows the results of combining the two approaches to find the joint properties in intricate specimens.

2 Laboratory Experimentation

2.1 Sample preparation

Two sandstone samples of dimension 10cm x 5cm x 10cm are selected, and a circular hole of 2.1 cm is cored at the center of the sample to simulate a circular opening of a tunnel. To simulate the artificial joint, one sandstone sample is cut at 30° and another at 45° from the horizontal passing through the center of the specimen, cutting it in two halves as shown in Fig. 1. Finally, cut pieces of samples are pasted using a mixture of Portland cement and water in a ratio of 4:1 by weight.

2.2 Experimental Setup

The prepared sandstone samples with artificial joints are uniaxially loaded in compression using a servo-controlled UTM (Universal Testing Machine), and an LVDT (Linear Variable Differential Transformer) is used to measure the horizontal displacement of the sample as shown in Fig. 1.

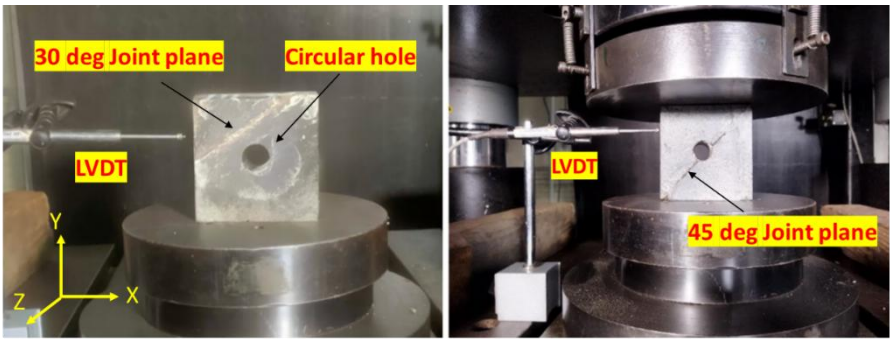

Fig. 1 Laboratory testing of sandstone samples (a) 30° joint, and (b) 45° joint.

The samples are uniaxially tested at a strain rate of 10^{-5}/sec. The LVDT is fixed at the left side of the upper block to measure the horizontal displacement of the jointed block. As the majority of displacement will be observed on the left portion of the specimen, to simplify the model the displacement so obtained by the LVDT is assumed to be the horizontal displacement of the block. The vertical load, vertical displacement, and horizontal displacement of the sample are recorded continuously by the data acquisition system. For 30° and 45° sandstone samples, compressive stress versus vertical displacement and compressive stress versus horizontal displacement of the samples are plotted in Fig. 2. The experiment was conducted until the sample failed. The maximum horizontal displacements of 30° and 45° samples are measured to be 1 mm and 1.77 mm, respectively. The intact rock properties of the sandstone specimen is determined in lab and elucidated in Table .

Table 1 Physicomechanical properties of sandstone

Parameters	**Value**	**Parameters**	**Value**
UCS (MPa)	222.86	Poisson's Ratio	0.29
Young's Modulus (GPa)	26.5	Density (kg/m^3)	2545

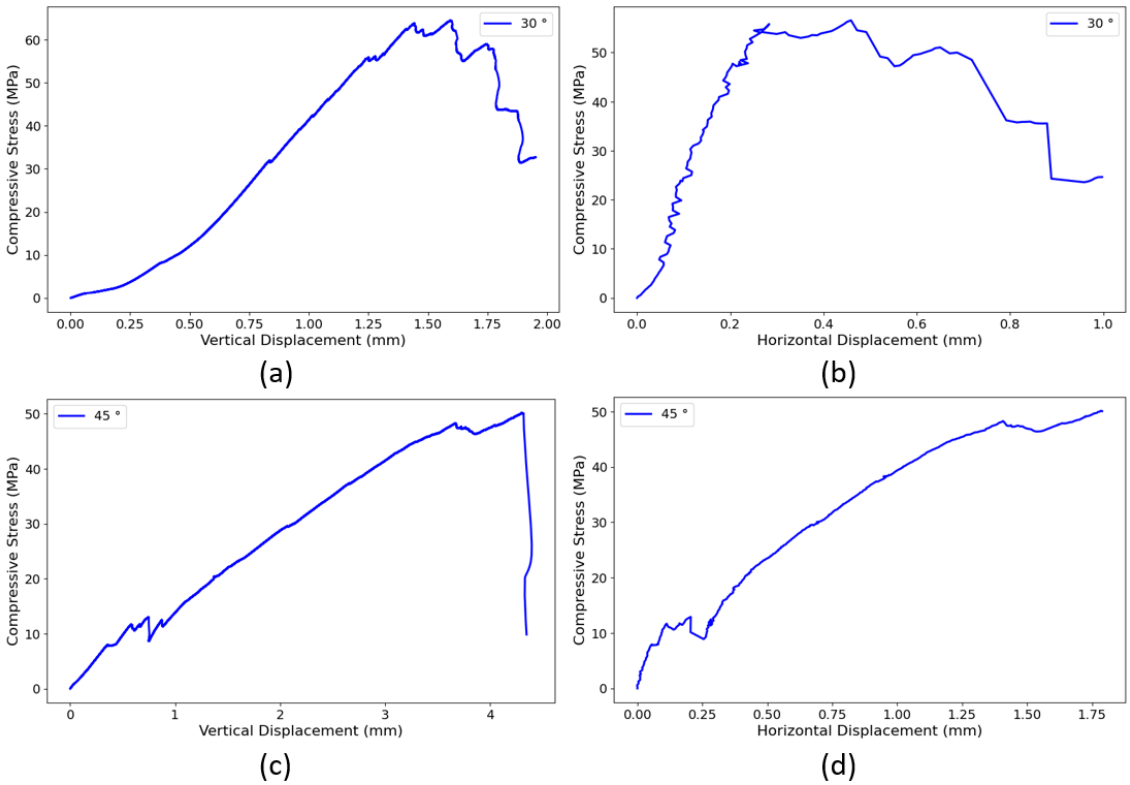

Fig. 2 Experimental plots of compressive stress versus vertical displacement and of compressive stress versus horizontal displacement of sample for 30° (a and b) and 45° (c and d) samples

2.3 Determination of shear and normal stiffness of the joint

For determination of shear stiffness and normal stiffness schematic diagram of applied stress and joint displacement is shown in Fig. 3. Where, σ_1 is applied normal stress on the sample, V is the vertical displacement of the sample, σ_n is normal stress on the joint plane, τ is shear stress on the joint plane, V′ is the vertical displacement (dilation) of the joint, U is the horizontal displacement of the sample, U′ is the displacement along the joint and θ is the angle of the joint.

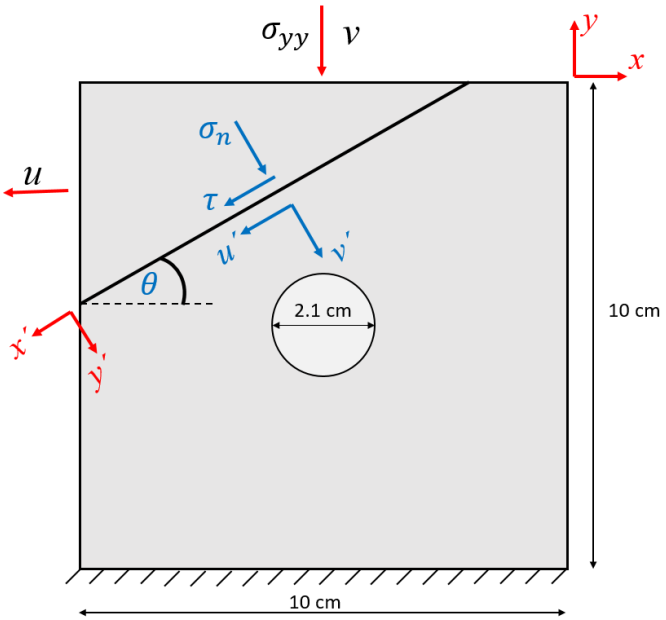

Fig. 3 Schematic diagram of applied stress and displacement on joint sample

Using the displacement transformation, if the axis is rotated with θ, the horizontal displacement and vertical displacement of the joint can be written as shown in Eq. (1 and

(2. Since the peak stress during the testing only reached to 0.25 times that of the UCS of the sample, the deformation of the rock is far less than that of the cement filling in the joint and the stresses are transformed assuming rock to be a rigid body. For a joint angle of 30°, $\theta = 210°$ and for joint angle 45°, θ = 45°. The following stress transformation equations are obtained in 2D,

$$U' = Ucos\theta + Vsin\theta \quad (1)$$

$$V' = -Usin\theta + Vcos\theta \quad (2)$$

Considering the average vertical stress applied by the servo-controlled UTM (σ_{yy}), by stress transformation, normal stress (σ_n) and shear stress (τ) along joint plane are found out as given in $\sigma_n = \frac{\sigma_{yy}}{2} + \frac{\sigma_{yy}}{2}\cos 2\theta = \frac{3\sigma_{yy}}{4}$ (3 and $\tau = \frac{\sigma_{yy}}{2}\sin 2\theta$ (4.

$$\sigma_n = \frac{\sigma_{yy}}{2} + \frac{\sigma_{yy}}{2}\cos 2\theta = \frac{3\sigma_{yy}}{4} \quad (3)$$

$$\tau = \frac{\sigma_{yy}}{2}\sin 2\theta \quad (4)$$

The graph between shear stress and displacement along the joint is plotted (Fig. 4 (a)) and the shear stiffness (K_{ss}) is found in joint samples. For normal stiffness (K_{nn}), the graph between normal stress and vertical displacement (Fig. 4 (b)) of the joint is plotted for joint samples. The joint properties, i.e., K_{ss} and K_{nn}, are determined as the slope of the linear portion of the graph, and values are reported in Table 2. These properties are used as essential input parameters for the joint in the FEM model in RS3.

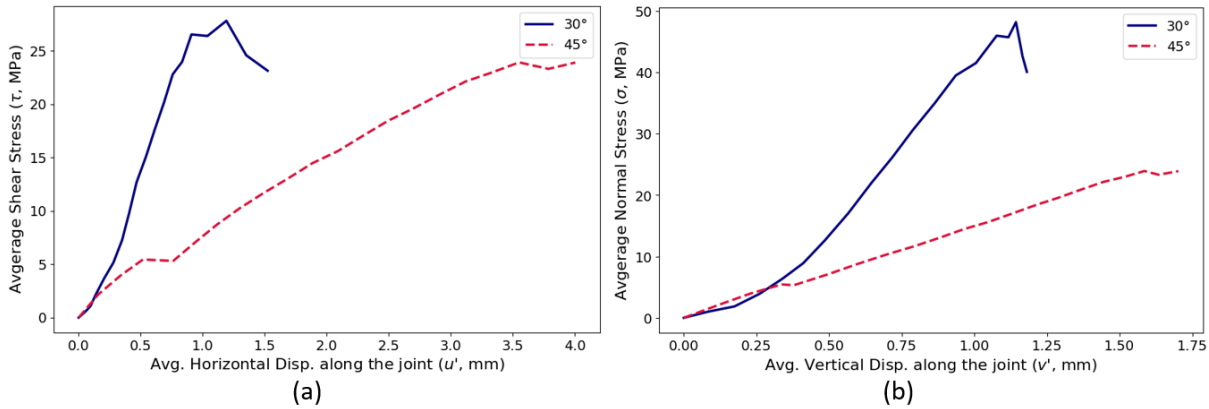

Fig. 4 (a) Average shear stress vs average horizontal displacement, and (b) Average normal stress vs average vertical displacement along the joint

3 Numerical Modelling

The experimental conditions are simulated using using RS3 software developed by Rocscience. RS3 is an advanced tool for geotechnical and rock mechanics engineers, facilitating the 3D Finite Element Method (FEM), and it enables detailed analysis of the mechanical behavior of joints and rock masses. Cuboid dimensions are the same as that of the experimental sample that was created. A circular hole with a diameter of 2.1 cm was added to the models. The joint is added to the model with the same joint angles. The material properties of sandstone samples and joints are assigned in the model, and the M-C failure criterion is used for analysis. The properties of sandstone as obtained from laboratory testing of the intact rock specimen and joint stiffness calculated from the elastic region of the average deformation versus the average stress curve in Fig. 4 are given in Table . The dilation angle of the joint is taken to zero to simulate the plane joint conditions.

Table 2 Material properties of sandstone and joint

Property of Sandstone	**Values**
Young's Modulus (GPa)	26.50
Poisson's ratio	0.29
Peak cohesion (MPa)	40.68
Peak friction angle (°)	50
Peak tensile strength (MPa)	0.008
Dilation angle (°)	0
Property of Joint	
Tensile strength (MPa)	0
Peak cohesion (MPa)	0.2
Peak friction angle (°)	35
Dilation angle (°)	0
Shear stiffness, K_{ss} (MPa/mm)	
30° joint sample	38.06
45° joint sample	7.20
Normal stiffness, K_{nn} (MPa/mm)	
30° joint sample	59.60
45° joint sample	15.07

The model is a plane stress problem with the Dirichlet boundary condition applied at the bottom face of the sample restraining its Z displacement to simulate the experimental conditions while the sides of the sample are free to move. The vertical displacement, as obtained by the UTM, is applied as the Neumann boundary condition at the top face in twenty incremental stages. The boundary condition of the model for the 30° sample is illustrated in Fig. . In numerical modeling, graded mesh and 35000 four-noded tetrahedral elements are used for the analysis.

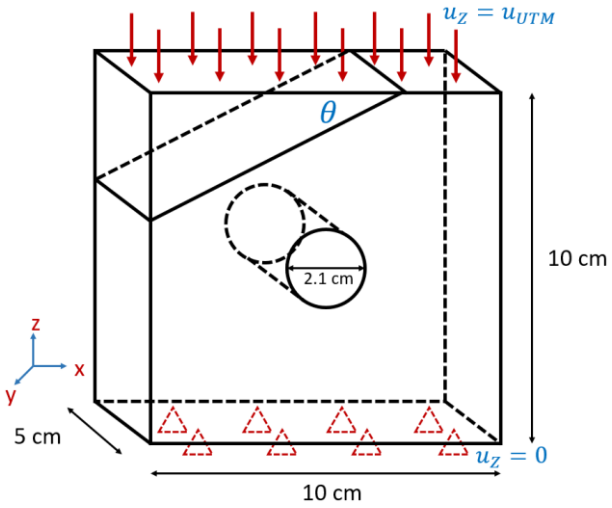

Fig. 5 Model dimension and boundary conditions

4 Result and discussions

The objective of the study is to find out the value of the cohesion and internal angle of friction along the joint for which experimental and numerical horizontal displacement of the sample (U) are matched with minimal error. In numerical results, the horizontal displacement of the sample (U) is measured using the query line option at the same location where the LVDT was positioned on the sample during experiments. For particular values of cohesion and friction angle along the joint, the horizontal displacement of samples as obtained from the simulation was recorded and compared with the corresponding experimental measurements, and the root mean square error (RMSE) was calculated. The cohesion and friction angle are determined by using the Bisection method until a set threshold value of $<$ 10 % RMSE is achieved. For 30° and 45° joint samples, the results of joint properties are shown in

Table .

Table 3 Values of the joint properties with their corresponding RMSE

Sample no.	Joint angle	Cohesion (kPa)	Friction angle	RMSE (%)
1	30°	200	35	6.21
2	45°	75	35	7.93

At these properties of the joint, the horizontal displacement of the sample (U) is plotted with the vertical displacement of the sample (V), as shown in Fig. .

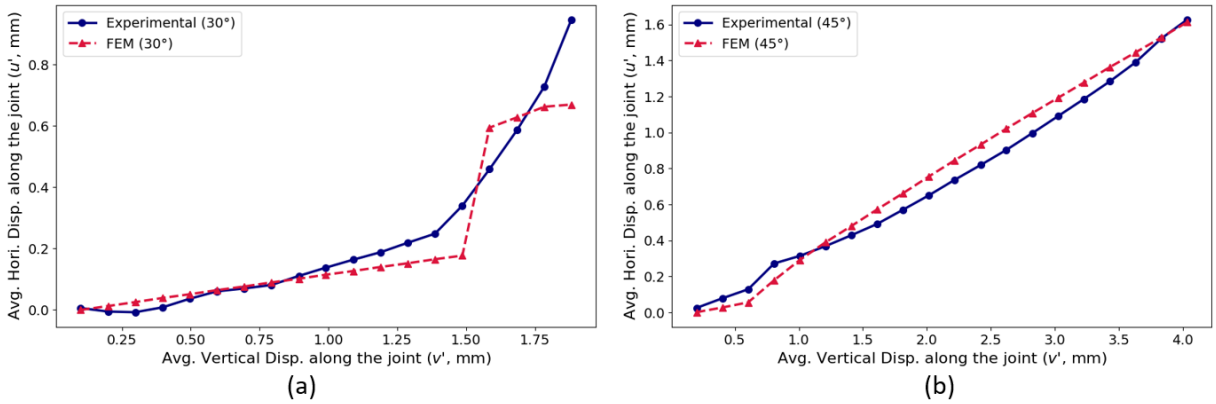

Fig. 6 Comparison of average horizontal and vertical displacements of sample of (a) 30º, and (b) 45º sample as obtained by the experiment and numerical model

The relative shear displacement along the joint plane is determined for the samples, as shown in Fig. . It is found that the max shear displacement is 0.0017 m and 0.000018 m for the 30° and 45° joint samples, respectively.

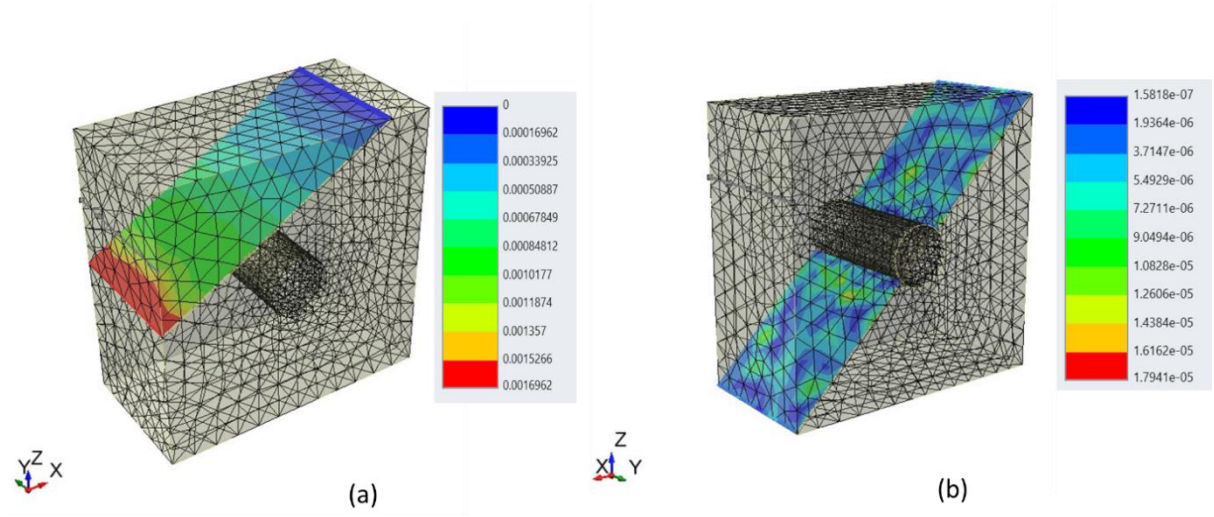

Fig. 7 Relative shear displacement (m) along joint for (a) 30°, (b) 45° joint model

To access the influence of the hole in the shear stress development along the joint, mean shear stress is calculated along the joint plane and is plotted in Fig. . For the 30° joint model, the shear stress tends to decrease in the region closer to the hole. Initially, it increases as the Euclidian distance from the centre of the hole increases in both directions (Fig. (a)). The shear stress decreases and minimizes at the maximum distance from the hole. For the 45° joint model, the shear stress at the hole's periphery is minimal, and a spike is observed in the region in close to the hole ($x < r$). Following the spike, the far-field shear stress tends to stabilize. The trend of the shear stress in both cases is in conjunction with the theory available in the literature for elastic stress development along the plane of weakness in the vicinity of underground openings (Deb, 2016; Brady and Brown, 2006).

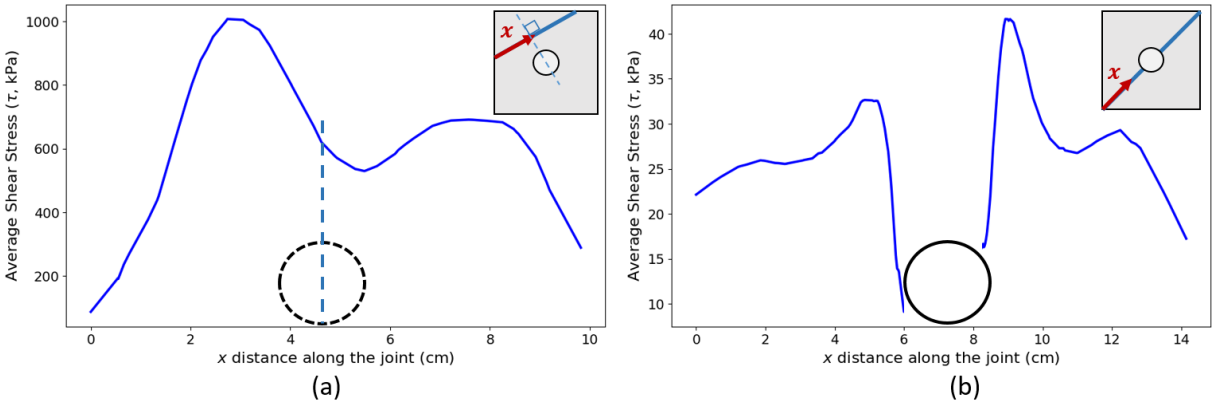

Fig. 8 Average Shear stress along joint plane for (a) 30°, and (b) 45° joint model

5 Conclusion

An experimental study on sandstone samples containing a circular hole is conducted. The joint plane at an angle of 30° and 45° are artificially made in the samples. The shear and normal stiffness of the rock joint are estimated by resolving the displacement measured by LVDT and UTM along the joint plane. For the 30° sample, shear stiffness and normal stiffness were found to be 38.06 MPa/m and 59.60 MPa/m, respectively, while for the 45° joint sample, shear stiffness and normal stiffness were found to be 7.20 MPa/m and 15.07 MPa/m, respectively.

To validate the obtained stiffness parameters of the joint plane, numerical modeling is performed using RS3 software. It is observed that the vertical and horizontal displacement of samples as obtained by the model are in close proximity to experimental results, which is evident from the low percentage of RMSE error (6.21 and 7.93 for 30° and 45° samples, respectively). The shear stress along the joint plane resembles the elastic stress distribution in the planes of weakness around circular openings. This shows the ability of the laboratory model to mimic the shear behaviour of rock joints around circular openings. Further, from the numerical model, the cohesion of 30° and 45° samples is found to be 200 kPa and 75

kPa, respectively. The internal angle of friction is found to be 35° along the joint plane for both cases. This study provides the approach of estimating the joint properties through numerical modeling for the cases in which direct estimation of these properties is difficult.

6 References

Aswad S, Wahyuwibowo DE, Qaidahiyani NF, et al (2020) Study on Influence of Joint Orientation on Rock Engineering Properties for Mining and Infrastructure Design. In: IOP Conference Series: Earth and Environmental Science. p 12001

Brady BHG, Brown ET (2006) Rock mechanics: for underground mining. Springer science & business media

Brown S, Scholz C (1986) Closure of Rock Joints. J Geophys Res 91:4939–4948. https://doi.org/10.1029/JB091iB05p04939

Daemen JJK, Danko G, Smiecinski AJ (2004) Experimental determination of stiffness of joints in welded Tuff

Dang W, Konietzky H, Frühwirt T (2017) Direct Shear Behavior of Planar Joints Under Cyclic Normal Load Conditions: Effect of Different Cyclic Normal Force Amplitudes. Rock Mech Rock Eng 50:3101–3107. https://doi.org/10.1007/s00603-017-1270-7

Deb D, Das K (2010) Extended Finite Element Method for the Analysis of Discontinuities in Rock Masses. Geotech Geol Eng 28:643–659. https://doi.org/10.1007/s10706-010-9323-7

Deb D, Verma A (2016) Fundamentals and Applications of Rock Mechanics

Dong S, Peng Y, Lu Z, et al (2022) Shear characteristics and shear strength model of rock mass structural planes. Sci Rep 12:13637

Fan L, Wei X, Wang M, Yang Q (2024) The investigation of joint stiffness determination based on the frequency characteristics of transmitted wave in rock mass. J Appl Geophys 222:105299. https://doi.org/https://doi.org/10.1016/j.jappgeo.2024.105299

Kumar R, Verma AK (2016) Anisotropic shear behavior of rock joint replicas. Int J Rock Mech Min Sci 90:62–73. https://doi.org/https://doi.org/10.1016/j.ijrmms.2016.10.005

Park J-W, Song J-J (2009) Numerical simulation of a direct shear test on a rock joint using a bonded-particle model. Int J Rock Mech Min Sci 46:1315–1328. https://doi.org/https://doi.org/10.1016/j.ijrmms.2009.03.007

Zhang Z, Zhu J, Deng J (2023) A comparative study for determining rock joint normal stiffness with destructive uniaxial compression and nondestructive ultrasonic wave testing. J Rock Mech Geotech Eng 15:1700–1712. https://doi.org/https://doi.org/10.1016/j.jrmge.2022.10.010